

INVESTIGATION OF ENTROPY NOISE IN AERO-ENGINE COMBUSTORS

Friedrich Bake*

Ulf Michel

Ingo Roehle

Division of Engine Acoustics
Institute of Propulsion Technology
German Aerospace Center (DLR)
Mueller-Breslau-Str. 8
10623 Berlin, Germany
Email: friedrich.bake@dlr.de

ABSTRACT

Strong evidence is presented that entropy noise is the major source of external noise in aero-engine combustion. Entropy noise is generated in the outlet nozzles of combustors. Low frequency entropy noise - which was predicted earlier in theory and numerical simulations - was successfully detected in a generic aero-engine combustion chamber. It is shown that entropy noise dominates even in the case of thermo-acoustic resonances. In addition to this, a different noise generating mechanism was discovered that is presumably of even higher relevance to jet engines: There is strong evidence of broad band entropy noise at higher frequencies (1 kHz to 3 kHz in the reported tests). This unexpected effect can be explained by the interaction of small scale entropy perturbations (hot spots) with the strong pressure gradient in the outlet nozzle. The direct combustion noise of the flame zone seems to be of minor importance for the noise emission to the ambiance. The combustion experiments were supplemented by experiments with electrical heating. Two different methods for generating entropy waves were used, a pulse excitation and a sinusoidal excitation. In addition, high-frequency entropy noise was generated by steady electrical heating.

INTRODUCTION

Combustion noise gains importance, especially during the landing approach of modern aircraft. This observation is mainly based on the achievements in decreasing jet mixing noise and fan noise of modern aero-engines.

The total noise radiated by a combustion chamber system consists of direct and indirect combustion noise as shown in a generalized acoustic energy equation by Dowling [1]. The direct noise sources are related to the unsteady combustion process itself, e.g. to unsteady heat release. The indirect combustion noise is generated when a fluid with a nonuniform entropy distribution is accelerated in or convected through the nozzle located at the downstream end of the combustion chamber. The accelerated or decelerated hot spots radiate sound. In gas turbines, the inlet guide vanes for the first turbine stage represent a nozzle for the combustion chamber flow. The flow in this nozzle is choked in aero-engines in practically all relevant operating conditions. The underlying theory of the acoustic mechanism is described by Marble & Candel [2]. In the following, indirect combustion noise (ICN) and entropy noise (EN) are used as equivalent expressions.

Up to now, there was little direct experimental proof of the existence of entropy noise in combustion with respect to the noise emission to the ambiance, presumably because of the difficulty to separate the different noise generating

*Address all correspondence to this author.

processes leading to entropy and direct combustion noise. Exceptions are the work in 1976 of Bohn [3] in which entropy waves and entropy noise were generated electrically and the experimental investigations of Muthukrishnan et al. [4] who separated the combustion noise sources via a coherence analysis.

The dispersion behavior of entropy fluctuations in a combustor flow was calculated by Sattelmayer [5]. Entropy waves are frequently studied with respect to their significance as a feedback force for combustion instabilities and thermo-acoustic oscillations, see e.g. [6–8]. However, the contribution to the noise emission of aero-engine combustors remained unknown. With the goal to evaluate the respective ratio of direct and indirect combustion noise, a model combustor and a reference test rig were set-up and acoustically investigated within the framework of a DFG research unit on combustion noise (<http://www.combustion-noise.de>). The results of this ongoing research work are presented in this paper.

EXPERIMENTAL SETUP

For the experiments two different test rigs have been used. The first one, called Entropy Wave Generator (EWG), is a nonreactive reference test rig to investigate the sound emission of artificially induced entropy waves in an accelerated tube flow. The second one is a model combustor test rig to demonstrate the noise emission of accelerated entropy perturbations in a reactive combustor flow.

Entropy Wave Generator (EWG)

The Entropy Wave Generator is basically an accelerated tube flow with the capability of inducing entropy waves via a heating module. The idea of this setup is to optimize and test detection methods for entropy noise. Furthermore, it allows to validate numerical (CFD + CAA) studies and to confirm theoretical considerations.

A sketch of the design is shown in Fig. 1. The flow, which is supplied by a compressed air system, is calmed in a settling chamber with a honeycomb flow straightener before it enters the tube section via a bell-mouth intake. The inner diameter of the tube is 30 mm. The heating module consists of six ring sections with ten platinum wires stretched through the cross section each. The wires have a diameter of 25 μm and a total length of about 1.2 m. In the current setup the wires can be heated with an electrical power of up to 200 W. The length of the heating module in streamwise direction amounts to 48 mm. The tube section following the heating module is exchangeable so that three different lengths, 42.5, 92.5 and 192.5 mm can be tested. Further downstream the flow is accelerated through the convergent

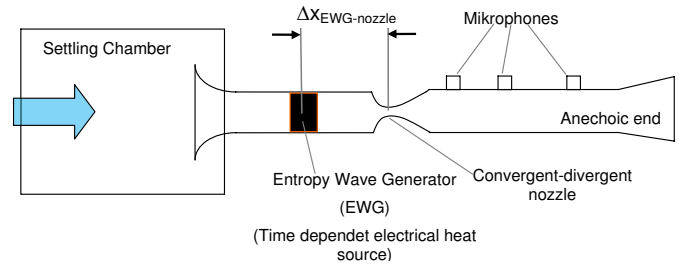


Figure 1. SKETCH OF THE ENTROPY WAVE GENERATOR (EWG).

part of a convergent-divergent nozzle and then decelerated in the subsonic divergent diffuser part of the nozzle. The following, 1020 mm long tube section has a diameter of 40 mm and is equipped with wall flush mounted microphones at different axial positions for acoustic analysis. The flow leaves the test rig through an anechoic termination in order to minimize acoustic reflections into the measurement section. The maximum mass flux limited by the air supply is 18 g/s and the maximum Mach number in the nozzle throat amounts to $\text{Ma} = 1$ at a mass flux of about 11 g/s and a nozzle diameter of 7.5 mm. A photo of the Entropy Wave Generator is displayed in Fig. 2.

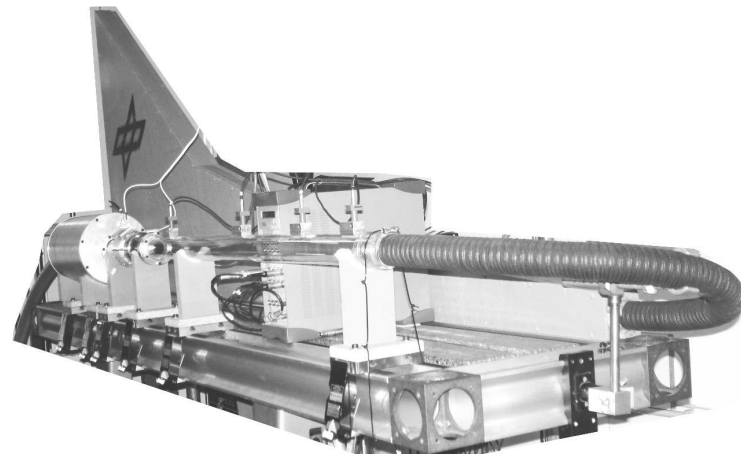


Figure 2. PHOTO OF THE ENTROPY WAVE GENERATOR (EWG).

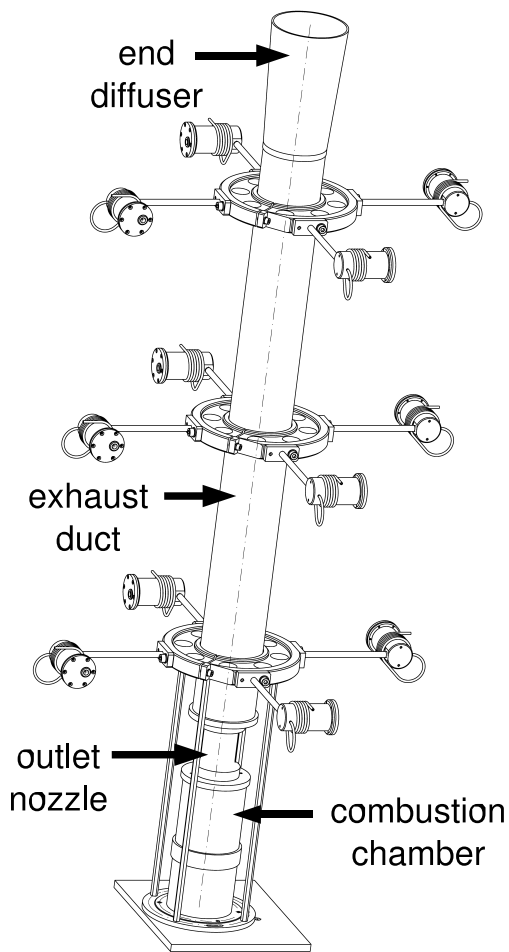


Figure 3. ISOMETRIC VIEW OF THE COMBUSTOR TEST RIG.

Combustor Test Rig Set-up

The combustor setup for the experimental investigation is chosen to replicate fuel-air-mixing characteristics of full scale gas turbines while still permitting analysis by experimental means. In order to simplify the acoustic analysis and the numerical approach, the system is designed axisymmetrically.

The test rig, shown in Figs. 3 and 4 consists of three sections: combustion chamber, outlet nozzle and exhaust duct. A swirled dual air-flow nozzle is used to drive the combustion zone. Methane gas is injected as the fuel through an annular slot between the air streams.

The combustion chamber itself is made of either a fused quartz glass or a stainless steel cylinder with 100 mm inner diameter. It has a length of 113 mm and is terminated by a convergent-divergent nozzle as shown in Fig. 4. The outlet

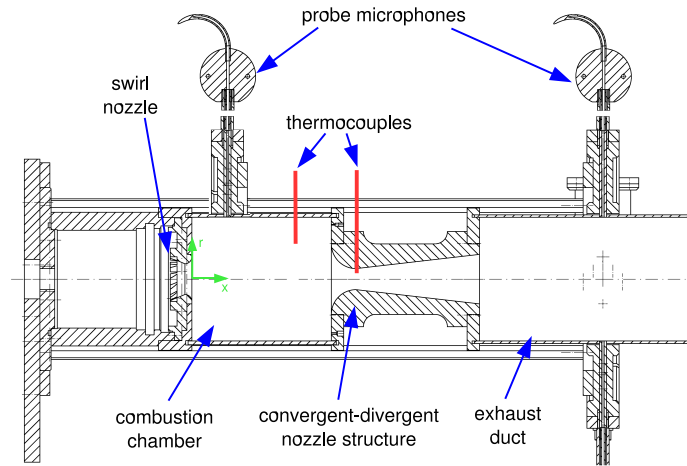


Figure 4. SKETCH OF THE COMBUSTION CHAMBER SETUP.

nozzle can be exchanged with nozzles of different throat diameters (7.5, 17, 20 and 30 mm) for testing the influence of the outlet Mach number on the indirect combustion noise.

The outlet nozzle is attached to an exhaust duct with the same diameter as the combustion chamber. In order to reduce the impedance jump at the exhaust outlet, an end diffuser is installed. In addition, the diffuser is perforated with holes of 2 mm diameter with increasing perforation density towards the exit. This exhaust duct termination is designed in consideration of the experimental investigations of Shenoda [9].

In order to excite the combustion process with perturbations, a piezoelectric device is installed in the fuel gas supply system to modulate the fuel mass flux dynamically. The fuel gas modulator is driven by a frequency generator.

Sound pressure measurements in combustion environments put high demands on the acoustic equipment. High temperatures of up to 2000 K and highly corrosive exhaust gases forbid the usage of normal microphone setups in the standard way. To prevent sensor destruction a probe microphone configuration like the one shown in Fig. 5 is used.

Due to the spatial separation of the measurement location at the combustion chamber wall or exhaust duct and the microphone itself, common 1/4-inch-microphones can be used. The connection between the exhaust duct wall and the microphone is realized by a steel tube of 2 mm inner diameter. For impedance matching and to minimize standing wave effects in the probe tube, this is extended according to the principle of the semi-infinite acoustic duct.

The microphone itself is perpendicular and flush-mounted inside the cylindrical chamber shown in Fig. 5.

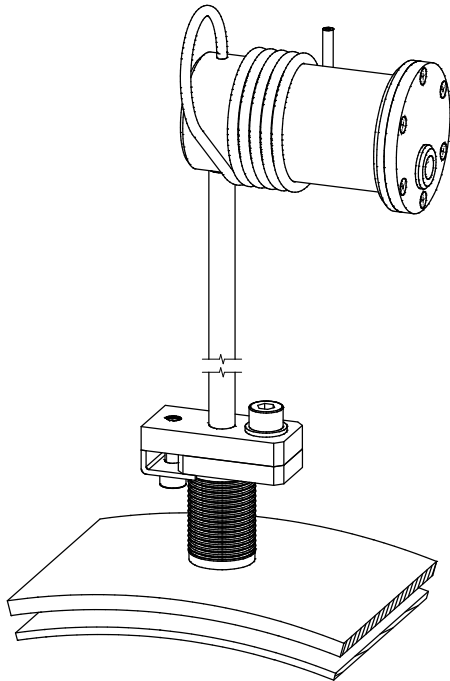


Figure 5. SKETCH OF THE PROBE MICROPHONE. THE MICROPHONE IS INSTALLED IN THE CYLINDRICAL PRESSURE CELL.

From the rear end, the probe tube is purged with cooling gas with a well controlled small flow rate. The purging prevents the diaphragm of the microphone from damage by corrosive combustion products. Of course, the phase shift in the collected data due to the propagation delay through the probe tube has to be corrected afterwards. Since the probe tube is finite, small reflection effects remain in the transfer function of the probe microphone. A detailed description of the calibrated transfer functions is given by Forster et al. [10].

In the current setup the combustion chamber can be equipped with up to three probe microphones at different axial positions. On the exhaust duct system twelve microphones can be installed at three axial and four circumferential positions. From the acoustic time-series, the downstream and upstream propagating acoustic waves can be determined using an inhouse processing code for mode analysis [11, 12]. Thus, the total sound power emitted by the combustion system can be determined. In the considered frequency range, the plane wave modes are the only propagating modes.

In order to obtain information about convecting temperature fluctuations or so called entropy waves, bare wire thermocouples with a diameter of $25 \mu\text{m}$ are installed in the combustion chamber and in the throat of the outlet nozzle.

For validation purpose and to map the flow field topology, the flow velocity field was measured using a quartz glass combustion chamber with square cross section and a three-component Laser-Doppler-System. Results were reported in [13], [14], and [15].

TESTS & RESULTS

The investigations meant to provide the evidence of entropy noise can be divided into three different approaches:

1. The time domain analysis of microphone signals in a pulse excitation mode. In the combustor setup the fuel gas supply is regulated by a piezo-electrical gas modulator. In the EWG rig the platinum wires are heated once per second, controlled by square-pulses from a function generator.
2. The cross-spectral analysis of microphone signals and either thermocouple signals in the combustor rig or excitation signals in the EWG, respectively, as a reference. For this the combustor rig is operated in a self-excited oscillating mode while the EWG is heated periodically.
3. By the spectral analysis of broadband entropy noise emission in a higher frequency range.

In the following the results of these three different approaches are presented for the combustor setup and the EWG rig, respectively.

Pulse Excitation

Combustor Test Rig: In the combustor test rig the non-sinusoidal excitation was implemented using a piezo-electric fuel gas modulator. Hereby, once per second the fuel gas supply was increased for a period of about 17 milliseconds. In the post-processing the microphone and thermocouple signals are phase averaged in reference to the excitation trigger signal. In this setup the thermocouple signal was acquired from the throat position of the convergent-divergent nozzle. The combustor was operated at a power of 9.05 kW and an equivalence ratio of 1.25 resulting in a mean bulk velocity of $\approx 1.2 \text{ m/s}$ in the combustion chamber. The Mach number in the combustor outlet nozzle was 0.5.

In the current work the thermocouple signals were not compensated. The associated amplitude loss is not of interest since the amplitudes are not further evaluated for the time domain and cross spectral analysis. With respect to the phase relation it is assumed that the regarded frequency ranges are above the cut-off frequency of the probe and therefore in a nearly phase constant region in the low-pass filter behavior of the thermocouples. Since only relative phase dependencies are regarded the absolute phase error is

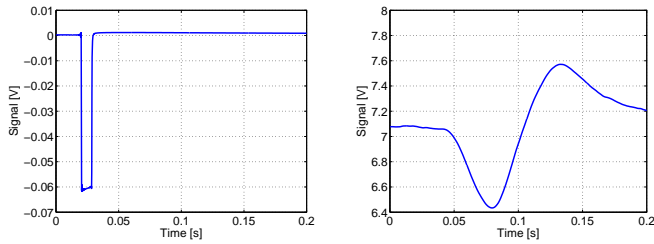


Figure 6. PHASE AVERAGED TIME SERIES OF TRIGGER (LEFT) AND THERMOCOUPLE (RIGHT) SIGNAL IN THE PULSE EXCITATION MODE.

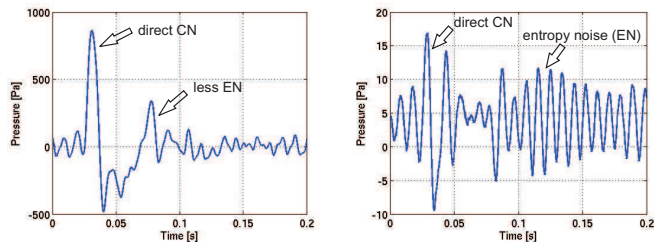


Figure 7. PHASE AVERAGED TIME SERIES OF COMBUSTION CHAMBER MICROPHONE (LEFT) AND EXHAUST DUCT MICROPHONE (RIGHT) SIGNAL IN THE PULSE EXCITATION MODE.

not relevant. However, the relative phase behavior of the thermocouples was determined using a chopped laser beam directed on the thermocouple junction and was found to be approximately constant for the here regarded frequency ranges.

Figure 6 shows the phase averaged time traces of fuel modulator trigger input on the left and of the thermocouple signal in the outlet nozzle on the right. After a delay period of about 50 milliseconds from the trigger pulse ($t_0 = 0.02$ s) the thermocouple indicates a distinct temperature modulation in the outlet nozzle with an amplitude of ± 0.6 V corresponding to a temperature fluctuation in the order of ± 50 K. The real temperature fluctuation is presumably much higher since uncompensated thermocouple data were processed here. Thus the triggered modulation of the fuel mass flux generates a perturbation of the heat release and with it a convecting entropy wave.

The phase averaged microphone signals are displayed in Fig. 7. Both the combustion chamber (left) and the exhaust duct (right) microphone show an intense pressure pulse shortly after the fuel trigger which corresponds to the direct flame response. The modulation in the fuel mass flux causes a fluctuation in the heat release which generates the primary propagating sound wave. But the fluctuation in the heat release also produces a downstream convecting entropy

wave, which creates in the outlet nozzle another pressure fluctuation indicated again in both microphone signals in Fig. 7. The convection time of about 50 ms fits to the mean flow velocity and the convection path in the combustion chamber from the flame to the nozzle. The effect of the two microphones in the combustion chamber and the exhaust duct being out of phase at the second pressure pulse series is also described in theory [2].

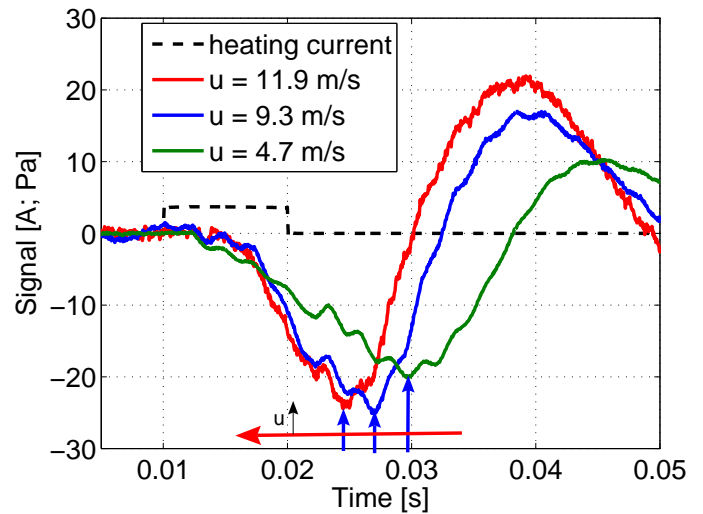


Figure 8. PHASE AVERAGED TIME SERIES OF ENTROPY-WAVE-GENERATOR MICROPHONE SIGNALS IN THE PULSE EXCITATION MODE AT DIFFERENT BULK VELOCITIES.

EWG: At the reference test rig the wires in the heating module of the EWG were electrically heated in the pulse excitation mode once per second with a pulse of ≈ 3.5 A at 77 V and a pulse duration of 10 ms. Under variation of various parameters like mean flow velocity, Mach number and distance between heating module (EWG) and nozzle ($\Delta x_{\text{ewg-nozzle}}$), microphone signals from positions upstream and downstream of the nozzle were acquired. In the post-processing analysis the signal traces were phase averaged using the current excitation signal as reference.

Figure 8 shows the phase averaged signals of a microphone downstream of the nozzle for different bulk velocities in the tube flow and therefore different Mach numbers in the nozzle. The heating current signal is also plotted in the graph as a dashed line. The entropy wave induced by the EWG generates a negative pressure pulse in the nozzle throat after a propagation delay. This pressure pulse then

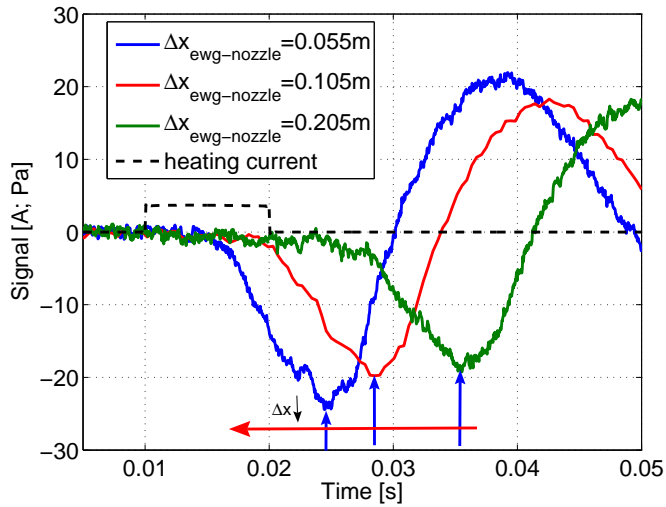


Figure 9. PHASE AVERAGED TIME SERIES OF EWG MICROPHONE SIGNALS IN THE PULSE EXCITATION MODE FOR DIFFERENT TUBE LENGTH Δx BETWEEN HEATING MODULE (EWG) AND NOZZLE.

propagates with the speed of sound and is recorded by the microphones downstream of the nozzle. It can be seen in Fig. 8 that the increase of the bulk velocity yields a corresponding decreased time delay and an increased pressure amplitude. The maximum Mach number at this measurement series was $Ma = 1$.

Figure 9 shows the time-domain averaged signals at different distance lengths between EWG and nozzle throat. For the measurements tube sections with different lengths have been inserted in the test rig. Here, the bulk velocity in the tube section was 11.9 m/s and the Mach number in the nozzle $Ma = 1$. The propagation delay of the entropy wave and the corresponding pressure pulse is equivalent to the changing propagation path between EWG and nozzle throat if the noise generating entropy waves are traveling with the mean velocity of the flow. The amplitudes of the pressure pulses decrease slightly with increasing duct length probably due to an increased dispersion of the entropy wave.

Sinusoidal Excitation

Combustor Test Rig: In general to determine the propagation speed of traveling perturbations measured by certain sensors at different positions, the phase relationships between the signals of these sensors have to be analyzed. First the cross spectrum between the two sensors has to be calculated. Then the phase relation in a frequency range of strong coherence between these two sensors has to be considered. A phase relation that is linear with frequency, stands for a propagating perturbation, whereby the slope of

the phase relation is anti-proportional to the propagation speed. Thus, at constant propagation path perturbations propagating with the speed of sound result in a much flatter phase line than perturbations traveling with flow velocity.

The combustion chamber setup was hereby operated in a resonant self-oscillating mode at a power of 8.35 kW and an equivalence ratio of 1.25. Signals from a thermocouple in the combustion chamber as well as microphone signals of the combustion chamber and the exhaust duct were acquired. The outlet nozzle diameter used was 7.5 mm, which yields an outlet Mach number of $M \approx 0.47$. The mean bulk velocity in the combustion chamber was ≈ 1.03 m/s

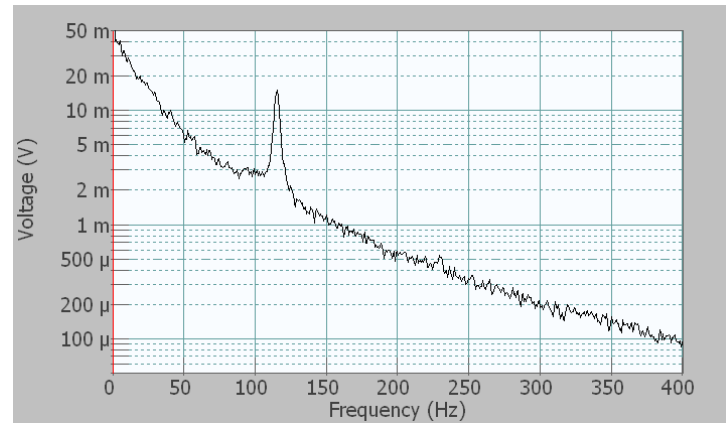


Figure 10. POWER SPECTRUM OF THE THERMOCOUPLE SIGNAL IN THE COMBUSTION CHAMBER IN A SELF-OSCILLATING MODE.

Figure 10 shows the power spectrum of the thermocouple in the combustion chamber at $x = 85$ mm and $r = 25$ mm with a clear peak at 115 Hz which is also found in the acoustic signals. This indicates the convection of hot spots with the resonance frequency of the system. To extract the phase relationship the cross spectral density function is evaluated between the thermocouple and the microphones in the combustion chamber and the exhaust duct, respectively. Figure 11 displays the zoomed cross spectra for the above mentioned self-oscillating resonance case.

Considering plane propagation modes the slope in a phase-frequency diagram is inversely proportional to the corresponding propagation speed. The difference between the curves of the two cross spectra in Fig. 11 is obvious. While the phase between thermocouple and combustion chamber microphone (green) shows a negligible slope, the phase relation between the thermocouple and the exhaust microphone (black) indicates a much steeper slope related to a distinctly lower propagation velocity. Regard-

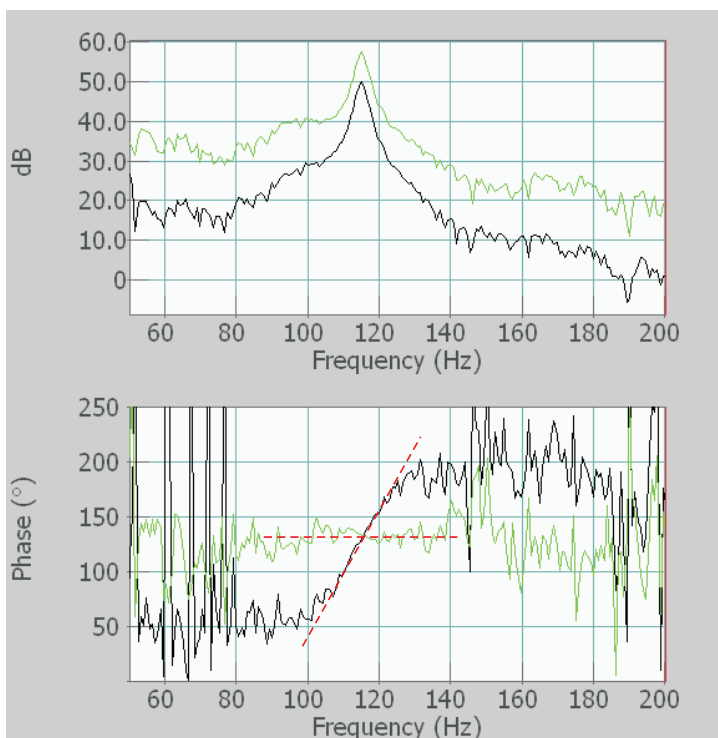


Figure 11. CROSS SPECTRA BETWEEN THERMOCOUPLE AND COMBUSTION CHAMBER MICROPHONE (GREEN) AND THE EXHAUST DUCT MICROPHONE (BLACK) AT A SELF-OSCILLATING MODE.

ing a propagation distance between the thermocouple and the convergent-divergent nozzle of 52.5 mm the phase relation results in a propagation velocity of approximately 3 m/s which matches the mean flow velocity in this region. In comparison the speed of sound in the combustion chamber is as high as 900 m/s. Thus, the temperature or entropy perturbation is convected with flow velocity from the primary combustion zone passing the thermocouple and accelerated in the outlet nozzle, where the entropy noise generation takes place. The latter is detected by the exhaust duct microphone. In contrast, the phase-frequency relationship between the thermocouple and the combustion chamber microphone (green) shows a phase that is almost independent of frequency, which indicates high propagation speeds.

EWG: At the EWG test rig a cross spectral analysis was conducted of measurements in a sweep excitation mode. Hereby, the EWG module was heated with a slow sweep over a certain frequency range. Since in this frequency range the microphone signals downstream of the nozzle indicate a strong coherence with the excitation signal and also ex-

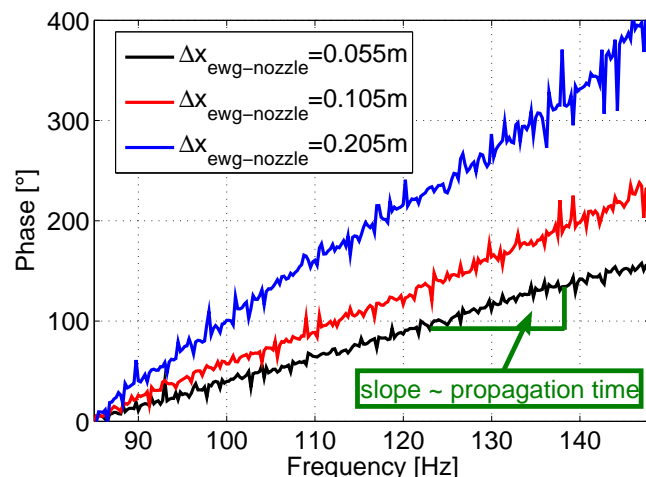


Figure 12. PHASE RELATION OF CROSS SPECTRA BETWEEN HEATING CURRENT AND MICROPHONE SIGNALS DOWNSTREAM OF NOZZLE FOR DIFFERENT TUBE LENGTH BETWEEN HEATING MODULE (EWG) AND NOZZLE.

Table 1. PROPAGATION VELOCITIES OF ENTROPY WAVES CALCULATED FROM PHASE RELATION IN COMPARISON WITH BULK VELOCITY OF THE FLOW FOR DIFFERENT TUBE LENGTH Δx BETWEEN HEATING MODULE (EWG) AND NOZZLE

Distance $\Delta x_{\text{ewg-nozzle}}$ [mm]	Time Delay [ms]	Propagation Velocity [m/s]	Bulk Velocity [m/s]
55	6.9	11.7	11.9
105	9.9	13.6	11.9
205	18.1	12.8	11.8

hibit a linear phase relation, the slope of this phase relation could be evaluated to provide the propagation velocity of the perturbations.

Figure 12 shows the phase plot of the the cross spectra between heating current and microphone signals downstream of the nozzle for an excitation sweep from about 85 to 145 Hz. The different traces correspond to different tube lengths between EWG and nozzle throat. The longest path distance ($\Delta x_{\text{ewg-nozzle}} = 205$ mm) results in the steepest phase line due to the same propagation velocity.

From this phase relation the propagation velocity can

be quantified like shown in Tab. 1. Here, the second column displays the time delays resulting from the slope of the phase relation at different tube lengths (column one). Considering the acoustic propagation time of the generated entropy noise the traveling speed of the entropy waves can be determined in column three. These phase velocities give a good agreement compared to the bulk velocity of the flow (column four). However, it has to be considered that the tube flow features a certain flow profile, where the bulk velocity, calculated from the mass flux, the tube cross-section and the mean density, is only a spatial mean value.

Broadband High Frequency Noise

Combustor Test Rig: Further measurements in the combustion test rig indicate another probable entropy related noise generation mechanism. Hereby, the microphone signals of the combustion chamber and the exhaust duct are compared.

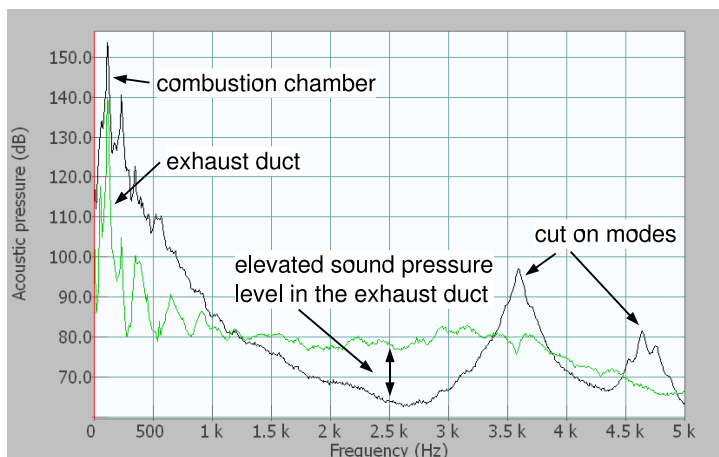


Figure 13. POWER SPECTRA OF COMBUSTION CHAMBER (BLACK) AND EXHAUST DUCT (GREEN) MICROPHONES UP TO 5 KHZ.

Figure 13 displays the corresponding power spectra in a frequency range up to 5 kHz. It demonstrates the increased sound pressure level of the exhaust duct microphone (green line) over the combustion chamber microphone (black line) in the frequency range between 1.4 and 3.3 kHz. The unsteady combustion process seems to create small scale entropy perturbations which generate high frequency broadband noise when accelerated through the combustion chamber outlet nozzle. A possible jet noise contribution in the exhaust duct yields much lower sound pressure levels due to the low mean flow velocity (≈ 2 m/s). Thus, jet noise can not be the reason for this elevated sound pressure level.

Above 3.5 kHz the spectrum of the combustion chamber microphone shows the appearance of higher acoustic modes, which are cut-off in the nozzle and cannot be observed in the exhaust duct. Since these higher order cut-on standing waves do not emit acoustic power, the dominating effect of broadband entropy noise in the exhaust duct system exists for all frequencies above 1.1 kHz. The operation conditions of this section were the same as in the previous one about the sinusoidal excitation.

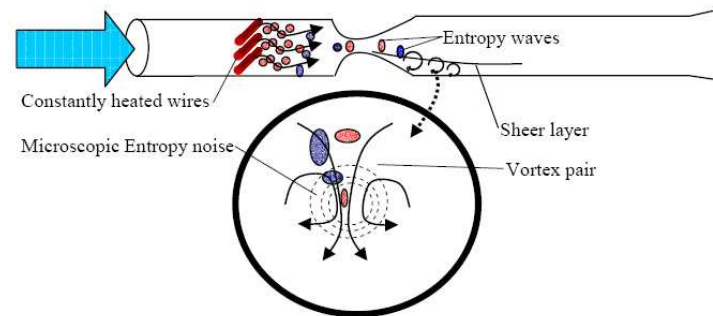


Figure 14. SKETCH OF NOISE GENERATION BY SMALL SCALE ENTROPY PERTURBATIONS IN THE ENTROPY-WAVE-GENERATOR AT CONSTANT HEATING.

EWG: In order to study broadband entropy related noise sources the EWG heating module was heated continuously in order to generate hot streaks in the wake of each wire. Since the distance between the heating module and the nozzle is comparatively small an equalization of these nonuniform temperature distribution does not occur. The authors are convinced that the strong acceleration of these temperature streaks and nonuniformities through the nozzle generates broadband entropy noise at higher frequencies. A sketch of this mechanism is shown in Fig. 14.

Figure 15 shows the power spectra of microphone signals downstream of the nozzle structure in the region from 500 to 3000 Hz. The blue line shows the reference case without heating at a nozzle Mach number of 0.35. The peaks in the spectrum are resonance frequencies of the flow system. The red curve displays the power spectrum with constant heating of all six wire sections. It is obvious that the sound pressure level is elevated in the heated case almost over the total frequency range. Especially in regions with lower background noise the augmentation of the total noise level by entropy noise amounts up to 7 dB in sound pressure level.

For a detailed quantification of the noise increase and

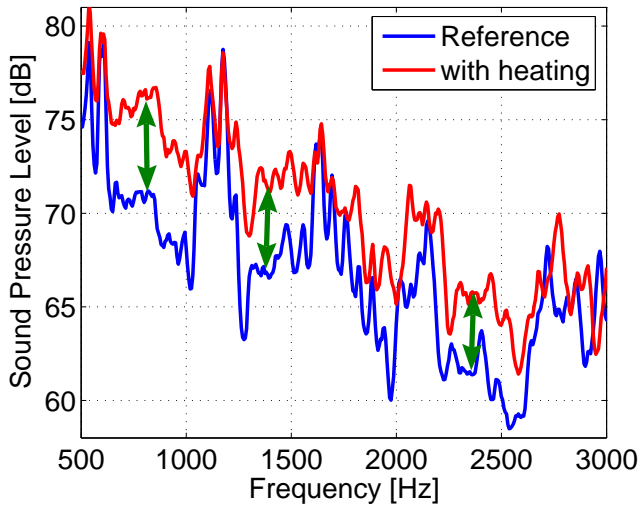


Figure 15. POWER SPECTRUM OF EWG MICROPHONE DOWNSTREAM OF THE NOZZLE WITH AND WITHOUT CONSTANT HEATING AT NOZZLE MACH NUMBER 0.35.

its dependency on the nozzle Mach number the frequency band power of the microphone signals between 1 and 4.5 kHz has been calculated at different Mach numbers for the non heated and the permanently heated case, respectively. In result Fig. 16 shows a strong non-linear increase in frequency band power difference with the Mach number. This observation supports the theory of Marbel & Candel [2], where a strong increase of entropy noise with the nozzle Mach number was predicted. In Fig. 16 the measured results can

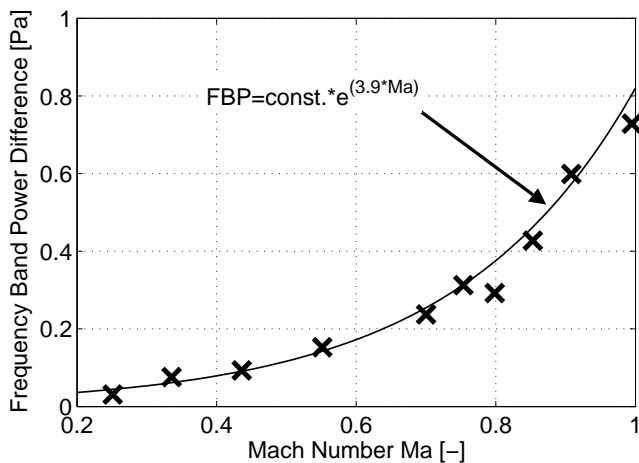


Figure 16. INCREASE OF FREQUENCY BAND POWER (1-4.5kHz) BETWEEN NON HEATING AND CONSTANT HEATING FOR CHANGING NOZZLE MACH NUMBERS.

be fitted by an exponential function, which underlines the strong Mach number dependence.

CONCLUSION

Entropy noise is generated when convecting entropy perturbations are accelerated through a nozzle at high Mach numbers. It was shown that entropy noise is the dominant source for the pressure fluctuations in the exhaust duct of a generic combustion chamber. The same conclusions can be drawn from experiments in a reference test rig (EWG) in which the entropy waves were generated by electrical heating.

Three different excitation schemes were applied in the electrically heated reference test rig. The results in a constant heating mode show the generation of broadband entropy noise at higher frequencies due to a spatially non uniform distribution of the temperature in the wakes of the heating wires. The entropy noise is shown to increase in amplitude with increasing flow Mach number as predicted theoretically.

The same effects including the high frequency broadband entropy noise in a well audible range between 1 and 3.5 kHz were found in the combustion test rig. It was shown that even at operating conditions with self-excited thermoacoustic oscillations the emitted sound power of the combustion system is related to entropy noise effects. So far, the nozzle outlet Mach number in the combustion rig reached only $Ma \approx 0.5$. Since the combustor outlet of aero-engines is choked in all relevant operation conditions and since the effect of entropy noise is expected to increase strongly with Mach number like shown in the reference experiment (EWG) it can be concluded that entropy noise will even be higher in real jet engines.

In aero-engines it can be assumed that additional entropy noise is generated in each turbine stage when the flow with nonuniform entropy passes the stages.

Considering the achievements in fan and jet noise reduction, the entropy noise mechanism requires further research activities especially with respect to the design of future aero-engine combustors to yield a more uniform temperature distribution in the outlet of the combustor.

ACKNOWLEDGMENT

The authors gratefully acknowledge the financial support by the German Research Foundation (DFG) through the Research Unit FOR 486 "Combustion Noise". We also would like to thank Sirko Niedworok for setting up and conducting the measurements at the "Entropy-Wave-Generator". Thanks go to Prof. Oliver Paschereit (TU Berlin) for his support of this work.

REFERENCES

- [1] Dowling, A. P., 1996. "Acoustics of unstable flows". In *Theoretical and Applied Mechanics*, T. Tatsumi, E. Watanabe, and T. Kambe, eds., Elsevier, Amsterdam, pp. 171–186.
- [2] Marble, F. E., and Candel, S. M., 1977. "Acoustic disturbances from gas non-uniformities convected through a nozzle". *J. Sound Vibration*, **55**(2), pp. 225–243.
- [3] Bohn, M., 1976. "Noise produced by the interaction of acoustic waves and entropy waves with high-speed nozzle flows". PhD thesis, California Institute of Technology, Pasadena, CA.
- [4] Muthukrishnan, M., Strahle, W. C., and Neale, D. H., 1978. "Separation of Hydrodynamic, Entropy, and Combustion Noise in a Gas Turbine Combustor". *AIAA Journal*, **16**(4), pp. 320–327.
- [5] Sattelmayer, T., 2000. "Influence of the combustor aerodynamics on combustion instabilities from equivalence ratio fluctuations". In *ASME Turbo Expo 2000*, no. 2000-GT-0082, ASME.
- [6] Polifke, W., Paschereit, C. O., and Döbbeling, K., 2001. "Constructive and destructive interference of acoustic and entropy waves in a premixed combustor with a choked exit". *The International Journal of Acoustics and Vibration*, **6**(3), pp. 135–146.
- [7] Eckstein, J., Freitag, E., Hirsch, C., and Sattelmayer, T., 2004. "Experimental study on the role of entropy waves in low-frequency oscillations for a diffusion burner". In *ASME Turbo Expo 2004*, no. GT2004-54163, ASME.
- [8] Eckstein, J., 2004. "On the mechanisms of combustion driven low-frequency oscillations in aero-engines". Dissertation, Technische Universität München.
- [9] Shenoda, F. B., 1973. "Reflexionsarme Abschlüsse für durchströmte Kanäle". Dissertation, Technische Universität Berlin.
- [10] Forster, S. F., Roehle, I., and Michel, U., 2004. Optimierung der passiven und aktiven Dämpfung von thermoakustischen Schwingungen. Abschlussbericht 4.4.2C, Deutsches Zentrum für Luft- und Raumfahrt, DLR, Berlin Charlottenburg. AG Turbo II - Verbundprojekt für ein CO₂-armes Kraftwerk.
- [11] Enghardt, L., Zhang, Y., and Neise, W., 1999. "Experimental verification of a radial mode analysis technique using wall-flush mounted sensors". In *137th Meeting of the Acoustical Society of America*, pp. 15–19.
- [12] Maier, R., Zillmann, J., Roure, A., Winninger, M., Enghardt, L., Tapken, U., Neise, W., Antoine, H., and Bouty, E., 2001. "Active Control of Fan Tone Noise from Aircraft Engines". In *7th AIAA/CEAS Aeroacoustics Conference*, no. 2001-2220.
- [13] Flemming, F., Olbricht, C., Wegner, B., Sadiki, A., Janicka, J., Bake, F., Michel, U., Lehmann, B., and Röhle, I., 2005. "Analysis of Unsteady Motion with Respect to Noise Sources in a Gas Turbine Combustor: Isothermal Flow Case". *Flow, Turb. Combust.*, **75**(1-4), December, pp. 3–27.
- [14] Duan, X. R., Weigand, P., Meier, W., , Keck, O., Stricker, W., Aigner, M., and Lehmann, B., 2004. "Experimental investigations and laser based validation measurements in a gas turbine model combustor". *Progress in Computational Fluid Dynamics*, **4**, pp. 175–182.
- [15] Duan, X. R., Meier, W., Weigand, P., and Lehmann, B., 2005. "Phase-resolved laser raman scattering and laser Doppler velocimetry applied to periodic instabilities in a gas turbine model combustor". *Applied Physics B / Laser and Optics*, **80**, pp. 389–396.